JOURNAL OF GEOPHYSICAL RESEARCH, VOL. 105, NO. D12, PAGES 15,403–15,416, JUNE 27, 2000

Influence of stratosphere-troposphere exchange on tropospheric ozone over the tropical Indian Ocean during the winter monsoon

M. Zachariasse,[1] P. F. J. van Velthoven,[1] H. G. J. Smit,[2]
J. Lelieveld,[3] T. K. Mandal,[4] and H. Kelder[1]

Abstract. Ozone (O_3) and relative humidity (RH) soundings, launched over the Indian Ocean during the 1998 winter monsoon (February–March), were analyzed. In the marine boundary layer (MBL), O_3 mixing ratios were relatively low (10–20 ppbv) except close to the Indian subcontinent (40–50 ppbv) where profiles were strongly influenced by pollution. Sometimes, relatively low O_3 levels were observed in the upper troposphere. These were associated with deep convection in regions where MBL O_3 levels were also low. In the midtroposphere (300–500 hPa), O_3 maxima (60–90 ppbv) were often found with low RH. A remarkable new finding of this study is that in more than a third of the profiles, laminae with very high O_3 mixing ratios (up to 120 ppbv) were observed just below the tropical tropopause (between 100 and 200 hPa). Back trajectory analyses showed that these layers originated in the vicinity of the subtropical jet stream (STJ). We hypothesize that stratosphere-troposphere exchange (STE) near the subtropical jet by either shear-induced differential advection or clear-air turbulence (CAT) caused the midtropospheric maxima (STE followed by descent) and the upper tropospheric laminae. Another new finding is that stratospheric intrusions were not only found near the STJ but also deep within the tropics. Given the thickness of the midtroposphere intrusions (typically 3–5 km) and the very high O_3 mixing ratios of the upper tropospheric laminae, it seems that STE plays an important role in the tropical tropospheric O_3 budget, at least over the Indian Ocean during the winter monsoon.

1. Introduction

Ozone (O_3) plays a key role in controlling the chemistry and climate of the tropical troposphere. Since it absorbs UV solar radiation, it is an important source for OH radicals. It is also an important greenhouse gas. Human activities increase the O_3 concentration of the troposphere through emissions from fossil fuel combustion and biomass burning [*Crutzen et al.*, 1979, *1985; Logan et al.*, 1981]. This will especially be the case in the future in the tropics where the economic activity is growing strongly with possible strong impact on chemistry and climate [*Intergovernmental Panel on Climate (IPCC)*, 1995, p. 109]. Simulations of the tropical tropospheric O_3 distribution are hampered by a lack of knowledge of transport processes such as deep convection, stratosphere-troposphere exchange (STE), and long-range transport from the source regions. The aim of this paper is to study how transport processes affect the tropospheric O_3 distribution over the Indian Ocean.

An important factor in transport studies is the lifetime of O_3. O_3 is photodissociated by short wave solar radiation (<340 nm) into electronically excited O (^1D) atoms. Reaction of these with water vapor forms OH radicals. Thus the lifetime of O_3 is basically determined by the amount of water vapor and solar radiation. The lifetime of O_3 increases from 2 to 5 days in the moist tropical marine boundary layer (MBL) to approximately 90 days in the free troposphere [*Fishman et al.*, 1991]. Thus, once O_3 is lifted from the boundary layer, it can be transported far away from its source regions. The tropical continental boundary layer (CBL) is an important source region of photochemically produced O_3. Biomass burning and fossil fuel combustion generate CO, CH_4, and nonmethane hydrocarbons. In a NO_x-rich environment the oxidation of these compounds produces O_3 [*Crutzen*, 1974; *Chameides*, 1978; *Fishman et al.*, 1979; *Crutzen et al.*, 1979, 1985; *Logan et al.*, 1981; *Greenberg et al.*, 1984; *Koppmann et al.*, 1997; *Chatfield et al.*, 1998]. Once it is vented from the CBL, this O_3 can be transported over large distances, as is shown by satellite and sounding measurements [*Krishnamurti et al.*, 1993; *Fishman et al.*, 1990, 1991; *Piotrowicz et al.*, 1989; *Baldy et al.*, 1996; *De Laat et al.*, 1999; *Thompson et al.*, 1996; *Chatfield et al.*, 1998; *Taupin et al.*, 1999]. The tropical MBL, on the other hand, is a sink region for O_3. *Kley et al.* [1996] have measured very low O_3 mixing ratios over the equatorial Pacific in the MBL as well as in the upper troposphere. Lifting of O_3-poor MBL air, with additional O_3 depletion that may occur in clouds, may have caused these minima [*Kley et al.*, 1996]. Similar minima have been found over the Indian Ocean due to lifting of O_3-poor MBL air by convective cells of the Intertropical Convergence Zone (ITCZ) [*De Laat et al.*, 1999; *Taupin et al.*, 1999]. An

[1]Climate Research and Seismology Division/Atmospheric Composition Research, Royal Netherlands Meteorological Institute (KNMI), De Bilt, Netherlands.
[2]Institute for Chemistry of the Polluted Atmosphere (ICG-2), Research Centre Jülich, Jülich, Germany.
[3]Institute for Marine and Atmospheric Research (IMAU), Utrecht University, Utrecht, Netherlands.
[4]National Physical Laboratory, New Delhi, India.

Paper number 2000JD900082.
0148-0227/00/2000JD900082$09.00

important source of O_3 in the tropics is also lightning. Since lightning creates a NO_x-rich environment in the atmosphere, O_3 production can occur [*Pickering et al.*, 1991; *Price and Rind*, 1994]. Lightning activity is mainly concentrated over the summer hemisphere landmasses in the tropics [*Price and Rind*, 1994]. Some photochemical ozone production also takes place in the tropical uppermost troposphere [*Folkins et al.*, 1999].

The stratosphere is a third source region through stratosphere-troposphere exchange (STE) by, for example, tropopause folds [*Shapiro*, 1980]. Exchange can also occur due to filamentation around the subtropical jet (STJ) [*Appenzeller et al.*, 1996; *Appenzeller and Holton*, 1997]. Shear-induced differential advection can cause tracer surfaces to stretch which leads to quasi-horizontal laminae-like tracer structures [see *Appenzeller and Holton*, 1997, Figure 1; *Ambaum*, 1997]. The mechanisms causing a tropopause fold and filamentation are, in principle, the same. The reason that we make a distinction between the two STE exchange mechanisms is because in foldings vertical tilting is important, whereas for the filaments stretching is more important so that they stay close to the tropopause. The mechanism we describe as filamentation is quasi-horizontal, chaotic mixing on a theta surface, which, in principle, conserves both theta and PV. Lastly, vertical shear in the strong shear zone near the STJ, by exceeding the Richardson number, can lead to clear-air turbulence (CAT), which is the third mechanism we distinguish [*Pepler et al.*, 1998; *Shapiro*, 1978; *Kennedy and Shapiro*, 1980]. The transport further into the tropics is again differential advection. STE is so far believed to play only a minor role in the tropical tropospheric O_3 budget [*Holton and Lelieveld*, 1996]. However, stratospheric intrusions have been found near the edges of the tropics, associated with tropopause folds in the vicinity of the subtropical jet stream [*Fabian and Pruchniewicz*, 1977; *Randriambelo et al.*, 1999; *Baray et al.*, 1998]. Apart from the studies from Pacific Exploratory Mission-West (PEM-West) and Measurements of Ozone by Airbus In-Service Aircraft (MOZAIC) [*Newell et al.*, 1996, 1999; *Browell et al.*, 1996; *Wu et al.*, 1997] and PEM-Tropics [*Fenn et al.*, 1999], other studies also indicated stratospheric influences in the tropical troposphere [*Krishnamurti et al.*, 1993; *Kley et al.*, 1996; *Suhre et al.*, 1997; *Cammas et al.*, 1998; *Taupin et al.*, 1999]. *Taupin et al.* [1999] found stratospheric intrusions into the upper troposphere near the edge of the tropics over the southern Indian Ocean during March and the austral winter (JJA). How far such stratospheric influences extend in the deep tropics needs to be studied in more detail.

To study the influence of transport on tropical tropospheric O_3 profiles, we analyzed O_3 and relative humidity (RH) profiles from the 1998 Indian Ocean Experiment First Field Phase (INDOEX FFP). To analyze air mass origins, we used back trajectories and meteorological data from the European Centre for Medium-Range Weather Forecasts (ECMWF).

2. Measurements

During February–March 1998, 14 O_3 and radiosondes were launched from the Indian research vessel *Sagar Kanya* over an extensive area of the Indian Ocean. A preliminary overview of the data is given by *Mandal et al.* [1999]. The ship track and location of the soundings are shown in Figure 1. The date and location of each sounding are presented in Table 1.

The sondes used were balloon-borne Electrochemical Concentration Cell (ECC) O_3 sondes (Model 1z, En-Sci Corp., Boulder, Colorado) coupled to Väisälä radiosondes (Model RS80-15 H, Väisälä, Finland). The uncertainties in the temperature and pressure measurements below 20 km are ±0.3°C and ±0.5 hPa, respectively. The accuracy of the humidity sensor (HUMICAP-H) varies from ±2% near the surface to ±15–30% between 5 and 15 km altitude [*Kley et al.*, 1997]. Above 15 km altitude the performance of the sensor is not reliable anymore [*Kley et al.*, 1997]. The accuracy of the O_3 sensor varies from ±1–2 ppbv below 5 km to ±5 ppbv at 10 km and ±20 ppbv at 20 km altitude [*Smit et al.*, 1994, 1998].

We categorized soundings according to their distance from the ITCZ (Table 1). The ITCZ position is estimated from the ECMWF vertical wind analyses at 500 hPa at a 1° × 1° horizontal resolution. The latitude range given for the ITCZ reflects its width and not the uncertainty in its determination. The categories are (I) far from the ITCZ (10° or more), (II) just north of the ITCZ (approximately 2°–5°), (III) just south of the ITCZ (approximately 2°–5°), and (IV) in or close to the ITCZ (within 1°).

3. Trajectory Model

Trajectories were calculated with the Royal Netherlands Meteorological Institute (KNMI) trajectory model [*Scheele et al.*, 1996]. The model uses ECMWF 6-hour forecast wind fields to calculate the displacement of an air parcel over a 1-hour model time step. Forecast data are used instead of analyzed data in order to rule out imbalances due to data assimilation in the model analyses. The data are available at 31 hybrid sigma-p model levels at a 1° × 1° horizontal resolution. For more details we refer to the User Guide to ECMWF Products 2.1 (1995, available from ECMWF).

For all calculations we applied clustered 5-day backward kinematic trajectories. We calculated multiple trajectories starting from 8 corners and 19 midpoints of the edges of a three-dimensional (3-D) box around the air mass of interest. The length, width, and height of the box are 1°, 1°, and 40–80 hPa, respectively. This cluster technique gives an impression of the reliability of the trajectories.

It cannot be excluded that the ECMWF analyses are inaccurate. The tropics is a data-sparse region, especially over the oceans, where the dynamics calculations are difficult due to a lack of a large-scale dynamical balance (such as the geostrophic balance for the extratropics) [*Heckley*, 1985]. ECMWF data postprocessing, as well as conversion from spherical harmonics space to grid point space, can also introduce errors. We believe, however, that ECMWF provides the best quality and finest resolution analyses around the world. In this study, we used data with a resolution similar to that of the model simulations. At this resolution the model resolves the larger convective cells of the ITCZ, although it probably underestimates the vertical motions herein. Subgrid-scale convection is not captured. Thus the actual path of an air parcel becomes unreliable if the trajectory passes through a convective area. This becomes important close to the ITCZ since individual turrets in the ITCZ are smaller than the model resolution. National Oceanic and Atmospheric Administration (NOAA) IR satellite pictures coincident with the trajectory locations were used to rule out the influence of convection as much as possible.

4. Analyses and Discussion of the Sounding Data

4.1. Description of the Soundings

Figure 2 shows the categorized profiles. In general, the profiles consist of multiple layers characterized by distinct maxima

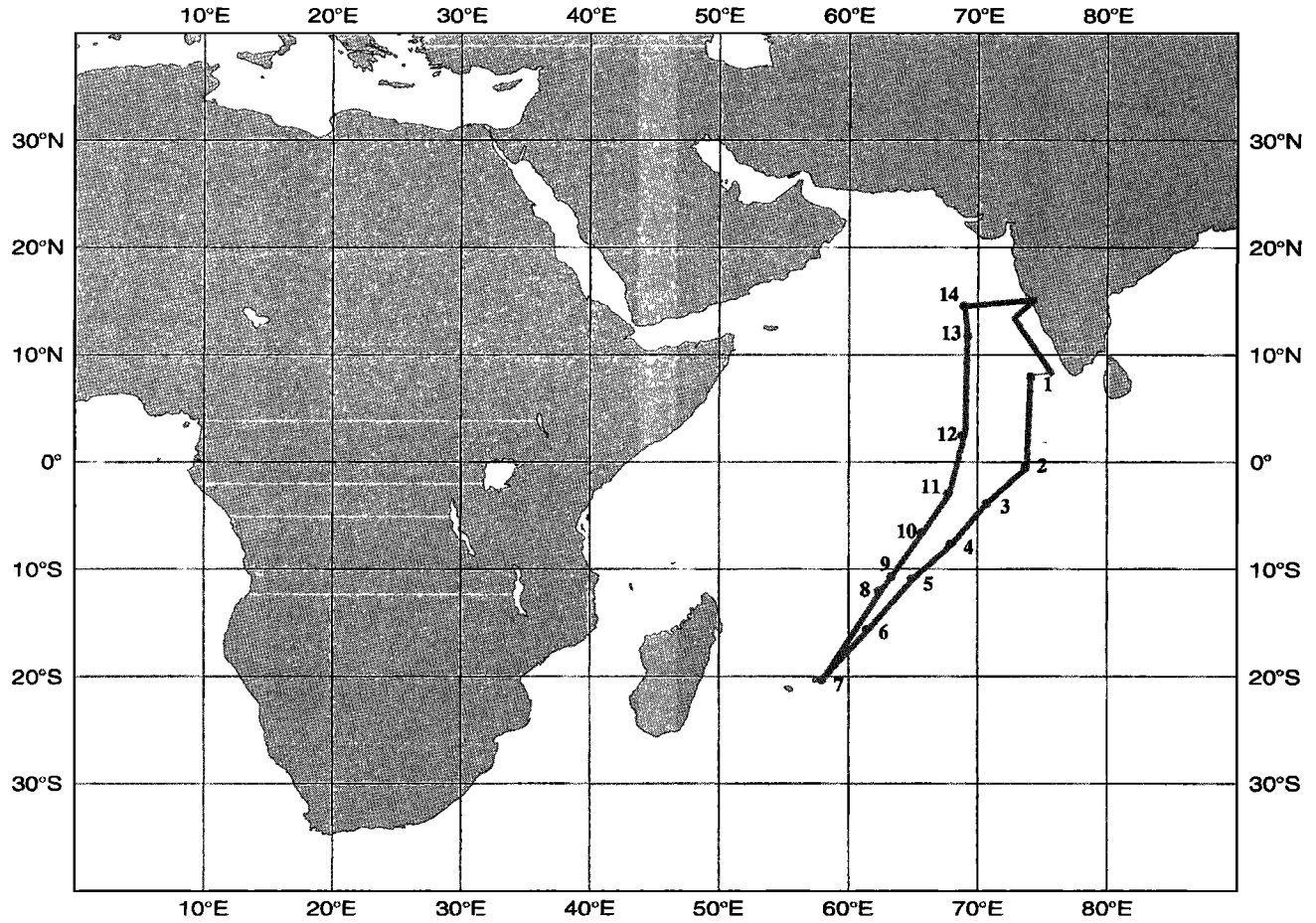

Figure 1. Shiptrack with the positions of the O_3 soundings. The first and last soundings were launched on February 23 and March 28, 1998, respectively.

and minima. Interesting features are very dry midtropospheric O_3 maxima (profiles 6, 7, and 12), upper tropospheric O_3-rich laminae (profiles 10–14), and upper tropospheric O_3 minima (e.g., in profiles 6 and 12). A detailed analysis follows in the sections below. In soundings just north of the ITCZ the lower troposphere has a layered structure superimposed on a 20-ppbv O_3 background. O_3 and RH are strongly anticorrelated. These layers are similar to those found in the MOZAIC and PEM data sets [*Newell et al.*, 1996, 1999; *Browell et al.*, 1996]. The average altitude of their layers was 5–6 km, to be compared to our altitude range, which was from just above the MBL to 7–8 km. The layer thickness is similar (about 1 km).

Table 1. Locations and Dates of the Soundings

Sounding	Date	Latitude	Longitude	ITCZ	Category
1	Feb. 23, 1998	8.0°N	74.0°E	3°–6°S	I
2	March 2, 1998	0.2°S	73.5°E	2°–5°S	II
3	March 4, 1998	4.3°S	70.2°E	8°–12°S	II
4	March 6, 1998	8.1°S	67.3°E	12°–17°S	II
5	March 8, 1998	11.1°S	64.5°E	12°–15°S	IV
6	March 10, 1998	16.1°S	61.0°E	12°–14°S	III
7	March 13, 1998	20.1°S	57.3°E	6°–8°S	I
8	March 18, 1998	12.4°S	62.5°E	4°–8°S	III
9	March 19, 1998	11.0°S	63.3°E	2°–7°S	III
10	March 20, 1998	7.1°S	65.2°E	3°–10°S	IV
11	March 22, 1998	3.0°S	67.3°E	5°S–2°N	IV
12	March 24, 1998	2.4°N	68.5°E	2°–10°S	II
13	March 27, 1998	11.4°N	68.8°E	0°–5°S	I
14	March 28, 1998	14.1°N	68.3°E	0°N–9°S	I

The soundings were launched either at the beginning of the afternoon or in the evening (local time). Also indicated is the position of the Intertropical Convergence Zone (ITCZ) and the categories into which the soundings were partitioned (see text section 2).

The MBL O_3 mixing ratios are generally low (10–20 ppbv), although slightly higher than those observed in 1995 [*De Laat et al.*, 1999]. Values as low as those over the equatorial Pacific [*Kley et al.*, 1996] are not observed here. MBL mixing ratios are enhanced to 40–50 ppbv close to India (soundings 1, 13, and 14). Trajectory analysis (for example, that for profile 13, see Plate 1a) shows that these elevated O_3 mixing ratios are due to photochemical O_3 production from Indian pollution outflow. A second outflow layer (800–900 hPa) overlies the MBL as shown by the trajectories of profile 13 in Plate 1b. The O_3 mixing ratios in this layer are even higher (70 ppbv) due to the longer lifetime of O_3 once it is in the free troposphere. The "background" free tropospheric O_3 mixing ratios are highest in the soundings close to the Indian subcontinent (50–80 ppbv). This is consistent with previous studies, which showed that the free troposphere can be influenced by continental boundary layer (CBL) pollution as a result of deep convective mixing [*Thompson et al.*, 1996; *Baldy et al.*, 1996; *Randriambelo et al.*, 1999; *Taupin et al.*, 1999; *De Laat et al.*, 1999]. The lowest MBL O_3 mixing ratios appear in the soundings just south of the

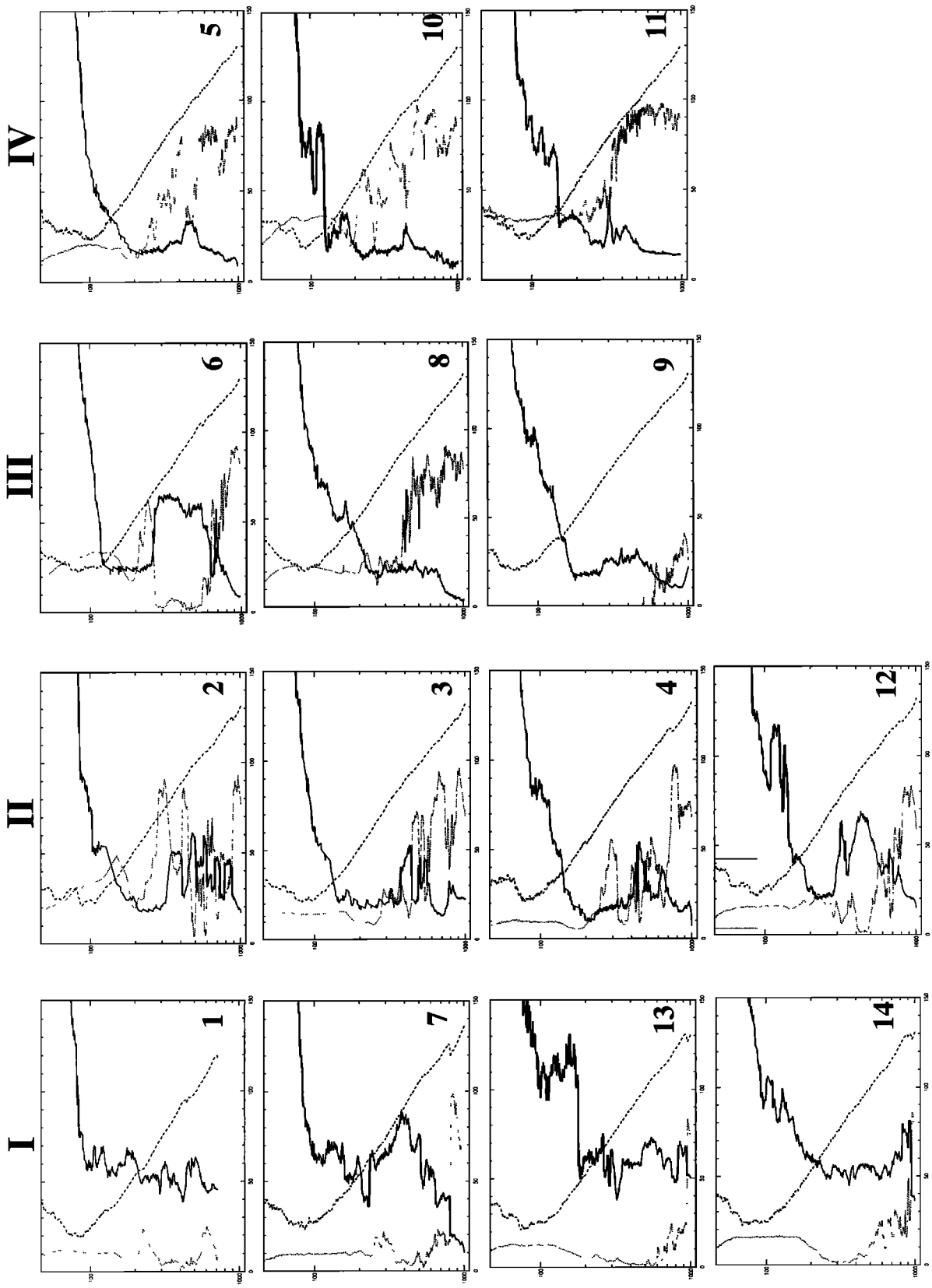

Figure 2. O_3, RH, and temperature profiles. Solid lines: O_3 (in ppbv), dotted lines: RH (in %), dashed lines: temperature (in K) offset by 170 K in order to fit into the plot. The horizontal axis runs from 0 to 150 (units: ppbv, %, and K). The vertical axis denotes the pressure from 1010 to 50 hPa. The soundings are classified into four categories depending on their position relative to the ITCZ: (I), from the ITCZ; (II), just north of the ITCZ; (III), just south of the ITCZ; (IV), in the ITCZ. The tropopause is indicated by the temperature minimum.

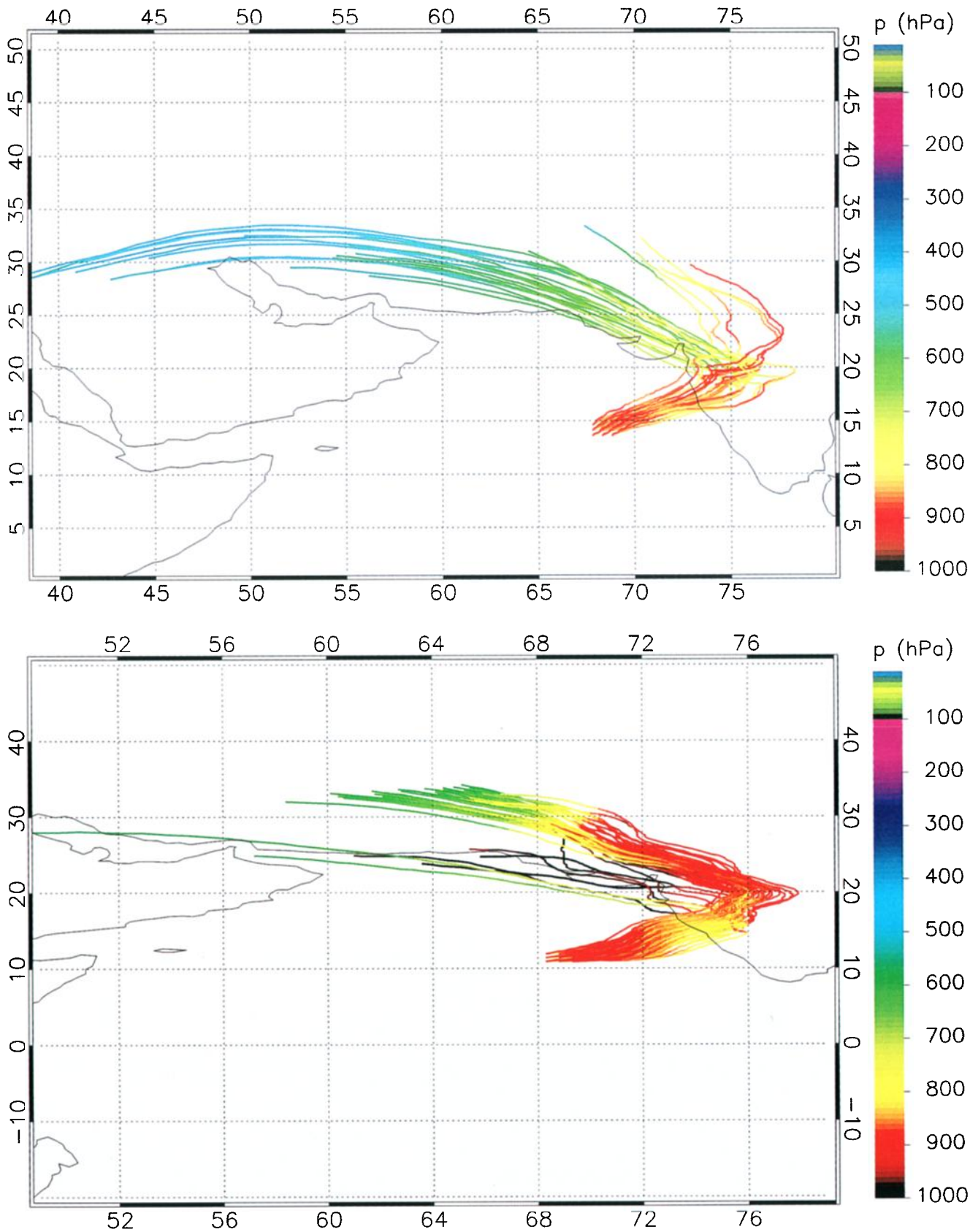

Plate 1. Five-day back trajectories from a 1° × 1° box surrounding the position of sounding 13. Trajectories end on March 27 at the following levels: (a) 920, 940, 960 hPa (in the MBL) and (b) 800, 820, 840, 860, 880 hPa (layer just above the MBL).

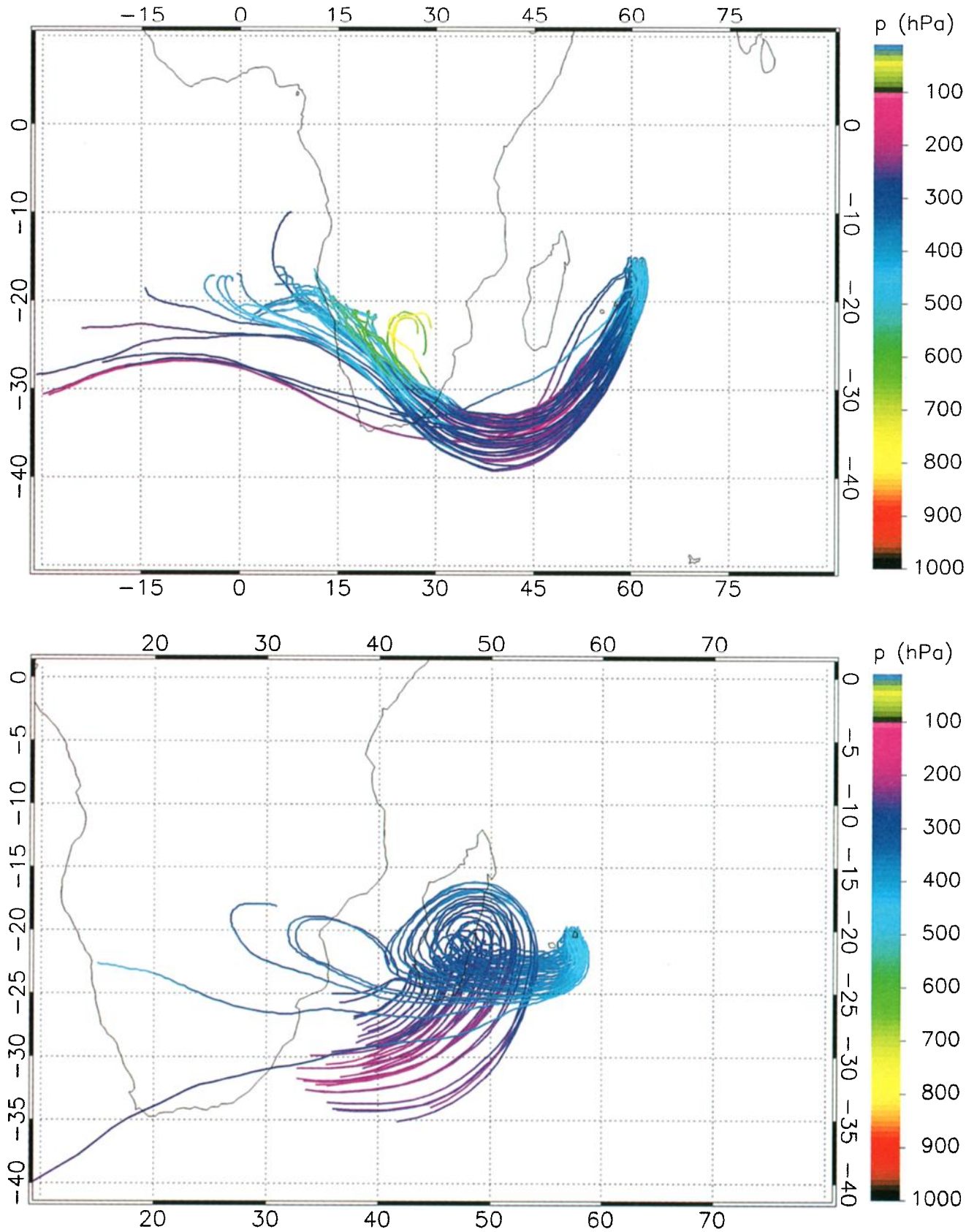

Plate 2. Five-day back trajectories from a 1° × 1° box surrounding the ozone maxima of soundings 6, 7, and 12. Trajectories end on the following days and levels: (a) March 10 (sounding 6) at 360, 380, 400, 420, 440, 460, 480 hPa. (b) March 13 (sounding 7) at 380, 400, 420, 440, 460 hPa. (c) March 24 (sounding 12) at 410, 430, 450, 470, 490 hPa.

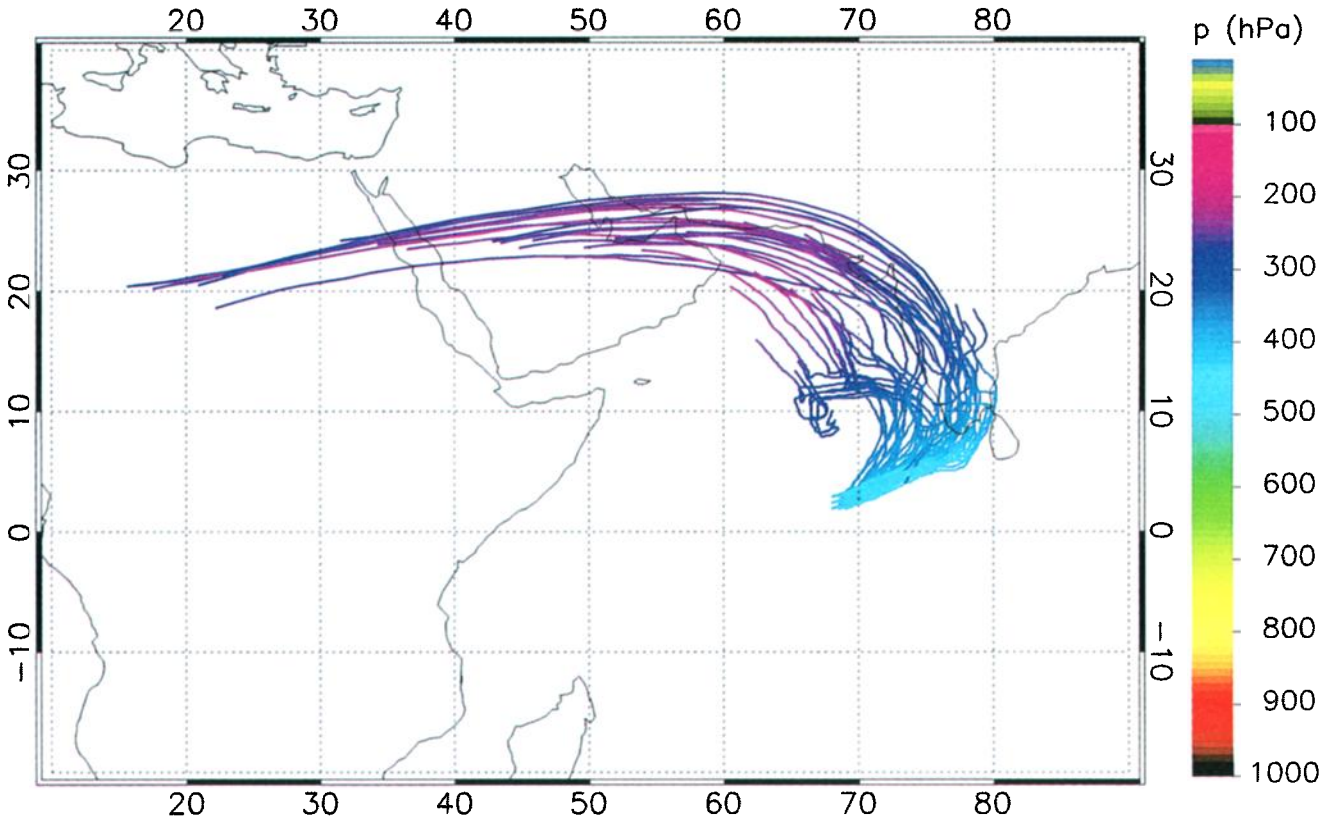

Plate 2. (continued)

ITCZ and in the ITCZ itself, reaching near-zero levels in soundings 4 and 8. We now analyze some of the general features in more detail.

4.2. Dry, Midtropospheric O_3 Maxima

The midtropospheric maxima in the profiles close to or in the ITCZ (5, 10, and 11) are a result of the convective activity. The lifetime of O_3 is short in the MBL. Convection vents O_3-poor air from the MBL to the upper troposphere [*Lelieveld and Crutzen*, 1994; *Roelofs et al.*, 1997; *Smit et al.*, 1991]. This O_3-poor air at upper levels is only slowly mixed back to lower levels by subsidence in the cloud-free part of the ITCZ. At midtropospheric levels the convective detrainment is often small. Thus O_3-poor air can develop in the upper troposphere and in the MBL, while the middle troposphere remains relatively unaffected. This results in a relative O_3 maximum in the middle troposphere.

The maxima in soundings 6, 7, and 12, which were released outside the ITCZ, have a different origin. These O_3 maxima are superimposed on background values of 20 ppbv and are extremely dry (RH < 5%). This dryness is also found in the ECMWF specific humidity analyses, of which a representative example is shown in Figure 3 for profile 6. The dry layer is part of a synoptic structure that slopes upward toward the STJ. The specific humidity analyses for profiles 7 and 12 are similar, with a dry layer at the location of the midtropospheric maximum. The fact that the model simulates a layer similar to that measured lends extra confidence to the back trajectory analyses, which are based on wind fields from this model.

The combination of high O_3 and low RH might be due to either a stratospheric origin or to convectively lifted CBL air that has subsided. Back trajectories show that the air masses in the maxima in soundings 6 and 7 (Plates 2a–2c) originated from the upper troposphere at 30°–40°S. Those for sounding 12 originated from 20°–30°N. These are exactly the locations of the STJ according to the horizontal wind analyses at 200 hPa (for example, Figure 4). A large vertical and horizontal shear zone surrounds this STJ, making this a favored region for STE. We therefore conclude that the maxima are most likely due to STE near the STJ. The influence of convective lifting of CBL air over India in sonde 12 was ruled out by comparison with NOAA IR satellite pictures. These showed no convective events during the period that the trajectories passed over India. India was still in the dry monsoon during that period, and large-scale subsidence prevailed. The extreme dryness of the layer in sonde 6 makes it highly unlikely that this air mass comes from the polluted CBL.

As described in the introduction, the STE can be induced by tropopause folds, shear-induced filament stripping from the STJ, or CAT followed by shear-induced differential advection. We did not find any evidence in the ECMWF data of tropopause folds in the sense of a deep vertically inclined frontal layer with high O_3 and PV and low RH. The explanation for the O_3 maxima is therefore probably one of the latter two STE mechanisms.

The RH decreases as the cluster further descends anticyclonically toward the deep tropics. During this descent the air has most likely mixed with tropospheric air since the O_3 values in the maximum are not purely stratospheric (70–90 ppbv compared to lower stratospheric values typically above 100 ppbv). A stratospheric PV signature along the trajectory could not be found for these O_3 maxima. In profiles 6 and 12, O_3

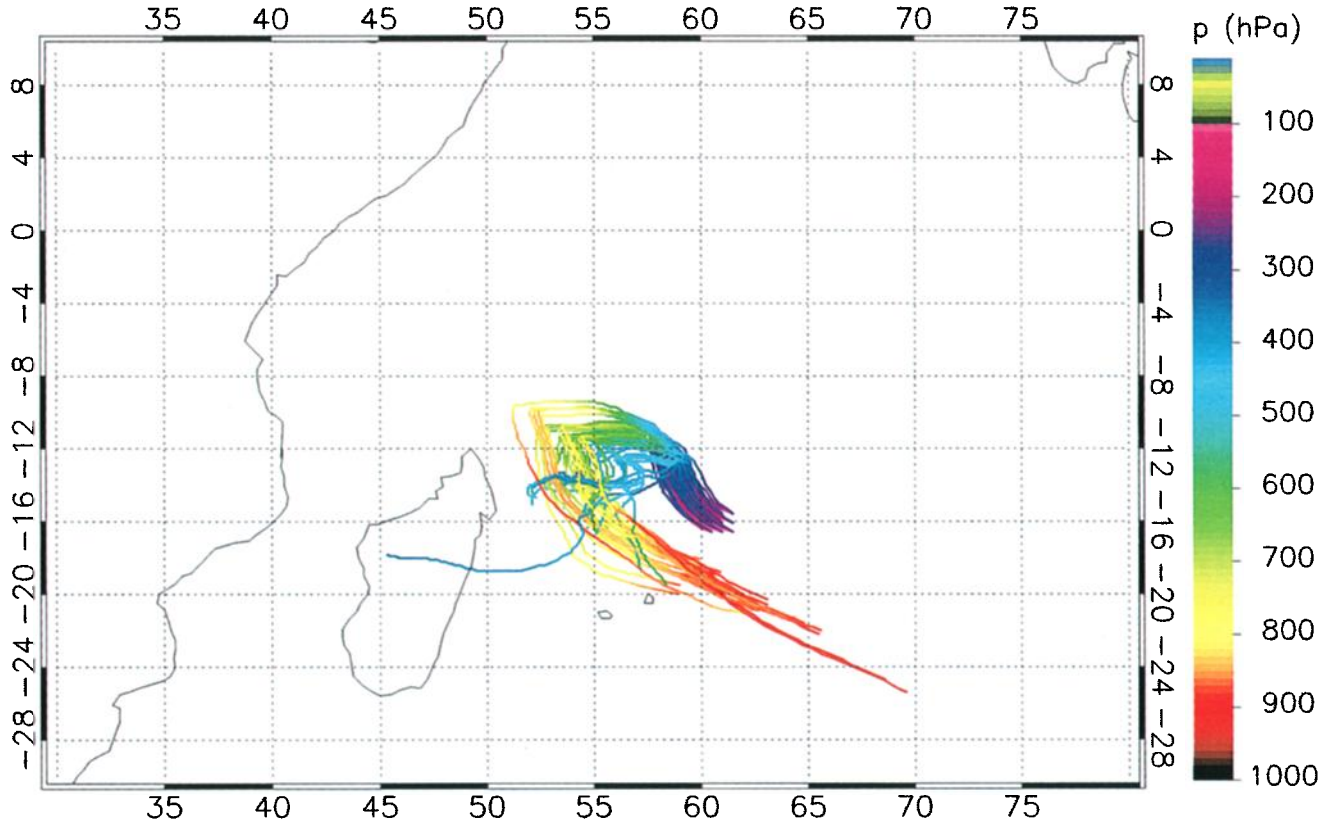

Plate 3. Five-day back trajectories from a 1° × 1° box surrounding the upper tropospheric ozone minimum of sounding 6. Trajectories end on March 10 at the following levels: 160, 180, 200, 220, 240 hPa.

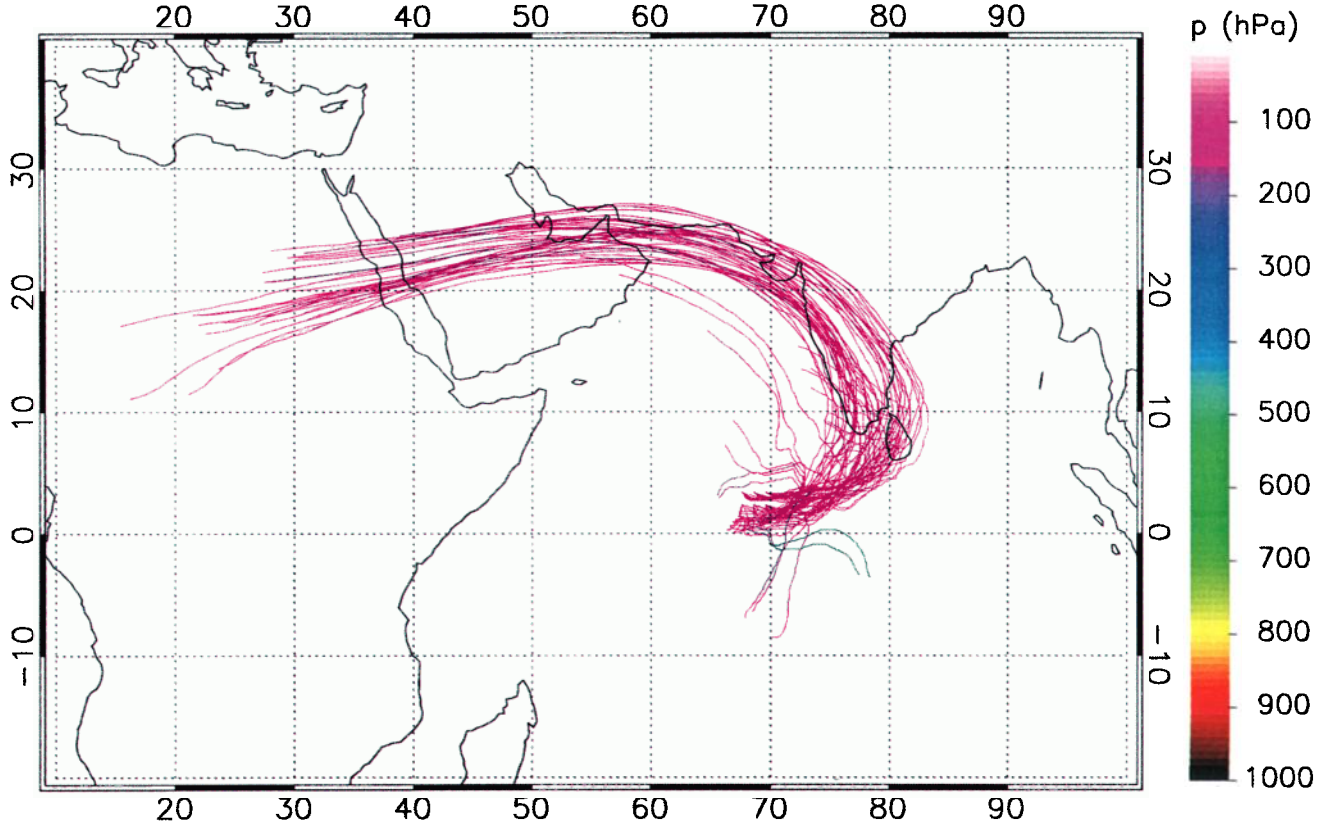

Plate 4. Backward trajectories starting from the upper tropospheric laminae of sounding 12. Trajectories from March 19–24 from 100 to 160 hPa at 10 hPa intervals.

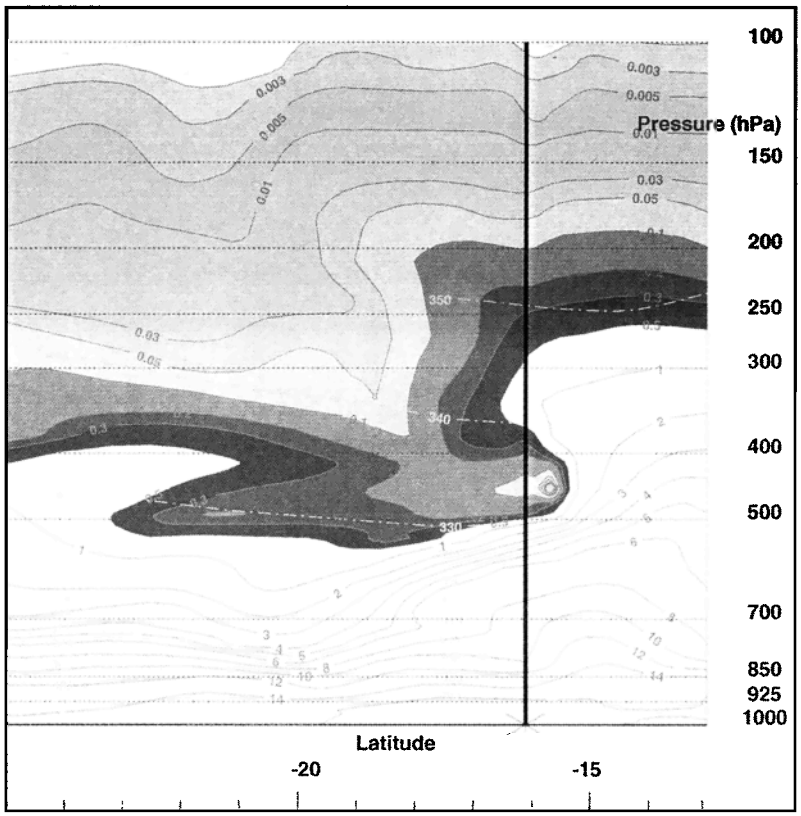

Figure 3. ECMWF specific humidity cross section (in g/kg) for profile 6 on March 10, 0600 UTC at 61°E. The position of the profile is indicated by the vertical line.

minima, with mixing ratios similar to near-surface values, overlie the midtropospheric maxima. Back trajectories from profile 6 (Plate 3) indicate that these air masses were lifted from the O_3-poor MBL. The ECMWF horizontal wind analysis (not shown) indicates that this vertical transport is caused by a cyclone-like perturbation, which involves rapid upward transport due to latent heat release. *De Laat et al.* [1999] show that these kind of upward motions are resolved (but probably underestimated) by the ECMWF data.

4.3. Upper Tropospheric Laminae

Trajectory analyses (of which a representative example is shown for profile 12 in Plate 4) indicate that most laminae originate near the STJ. After spending some time near the jet stream, the trajectories curve anticyclonically toward the equator. Similar to the midtropospheric maxima, we therefore expect that the O_3-rich laminae are the result of STE around the STJ. The analysis of the potential temperature (θ) along one of the trajectories of Plate 4 (at 110 hPa) corroborates the hypothesis of a stratospheric origin of these laminae (Figure 5). Since the tropical tropopause more or less coincides with the 380 K surface, the analysis shows that θ overshoots the tropopause value during the first few days. However, it must be kept in mind that the ECMWF vertical velocity field may have errors, which influence the θ evolution along the trajectory. Although the absolute change in θ (>10 K in <10 hours) is rather large, we have some confidence in the general trend of θ to decline over several days. Part of the temporal variations in θ is due to vertical interpolation errors of θ to the trajectory position.

Another indication of a stratospheric origin of the laminae of profile 12 is found in the PV map at 100 hPa (Figure 6a). A patch of typically stratospheric PV values is shown near the measurement site (the tropopause is defined by the 2 PVU contour). Laminae with stratospheric PV (and O_3) values appear to be stripped off the STJ (indicated also by following the filament a few days back, not shown) and transported anticyclonically along the trajectory paths over Sri Lanka and southern India to the measurement location. This stripping followed by transport toward the deep tropics is also observed in PV maps pertaining to other laminae. An example is sounding 7. Although not as pronounced as in the other soundings, a layer with elevated O_3 mixing ratios (70 ppbv) appears between 100 and 150 hPa. The corresponding PV map at 100 hPa (Figure 6b) shows a strongly meandering STJ. This meandering is accompanied by laminae stripping, evidenced by several tongues of stratospheric PV values (1.5–2 PVU) penetrating into the deep tropics and to the measurement site. Comparing the O_3 mixing ratios in laminae in the deep tropics to those close to the STJ, it seems that during transport mixing was not as important as for the midtropospheric ozone maxima. The layers can probably retain their identity for a long time because photochemical O_3 destruction is small in the dry upper troposphere and there may even be some O_3 production. We do not believe, however, that local production plays a major role in causing these layers in view of the evidence for STE presented above.

Another explanation for O_3-rich laminae might have been transport from the polluted CBL. However, it is most unlikely that low-level pollution creates stable layers with O_3 mixing

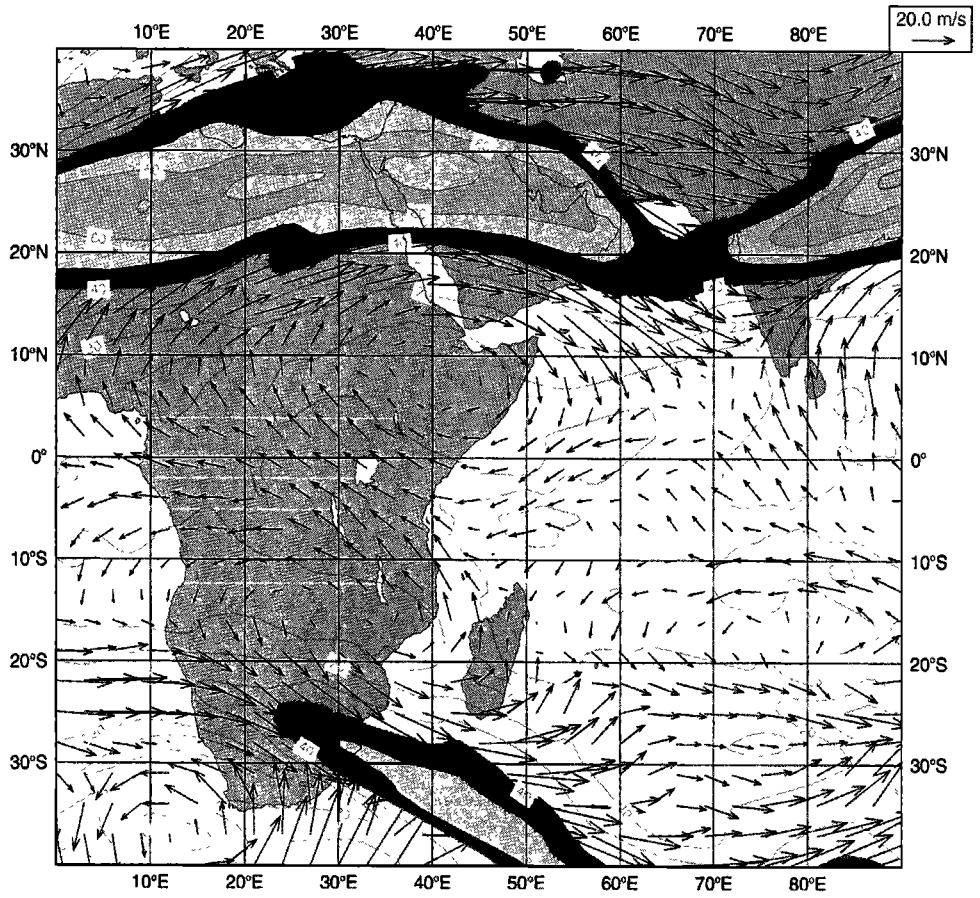

Figure 4. ECMWF horizontal wind and wind speed on March 10 (sounding 6) at 200 hPa. The Northern Hemisphere subtropical jet stream is stronger than the Southern Hemisphere jet stream.

ratios up to 120 ppbv in the upper troposphere. None of the trajectories showed any indication of recent contact with the polluted CBL since the entire cluster originates from the region of the STJ. The cluster remains in the upper troposphere during the 5-day period. Moreover, NOAA IR satellite pictures showed no convective events during the period that the trajectories passed over source regions such as India. This points to a stratospheric rather than a continental origin of the laminae.

Only a few of the trajectories from the laminae do not originate near the STJ (not shown). Instead, these seem to originate from the ITCZ. Yet also for these layers there are indications in the PV maps (not shown) that the air masses originate, at least partly, from the stratosphere.

5. Conclusions and Discussion

The picture that emerges from our analysis is that O_3 profiles over the Indian Ocean are often composed of several distinct air masses that cause alternating maxima, minima, and laminae in ozone. The observed profiles display the following features:

1. MBL mixing ratios are enhanced to 40–50 ppbv close to India due to outflow of pollution from the continent. MBL mixing ratios away from the Asian continent are relatively low (10–20 ppbv) consistent with efficient photochemical O_3 destruction. Convective lifting from the MBL can cause upper tropospheric O_3 minima.

2. There are elevated O_3 mixing ratios (50–80 ppbv) above the MBL originating from low-level outflow of polluted air from the Asian continent.

3. There are very dry midtropospheric maxima (60–90 ppbv) in the middle troposphere. We have presented evidence that this air most likely has a stratospheric origin.

4. There are high to very high O_3 mixing ratios (up to 120 ppbv) in laminae just below the tropopause. Also for these layers we have presented evidence of a stratospheric origin, with the STJ playing a central role in the exchange mechanism.

Stratospheric inputs have also been found in the tropics by *Newell et al.* [1996, 1999], *Browell et al.* [1996], *Wu et al.* [1997], and *Fenn et al.* [1999], but the repeated presence of stratospheric laminae just below the tropopause is a remarkable new finding of this study. Similar laminae are present in Central Equatorial Pacific Experiment (CEPEX) profiles over the central Pacific [*Kley et al.*, 1996], but they were not discussed by these authors. The laminae appear in more than a third of the profiles. We have shown with back trajectory analyses that the laminae originate from the vicinity of the STJ. We hypothesize that the STJ plays a central role in this STE mechanism either by directly shear-induced differential advection, which causes filamentation, or by CAT followed by differential advection. In principle, tropopause folds could also play a role, but we did not find evidence for these in the ECMWF data. Although the ECMWF data have a limited vertical and horizontal resolution, observed tropopause folds are often well captured by the

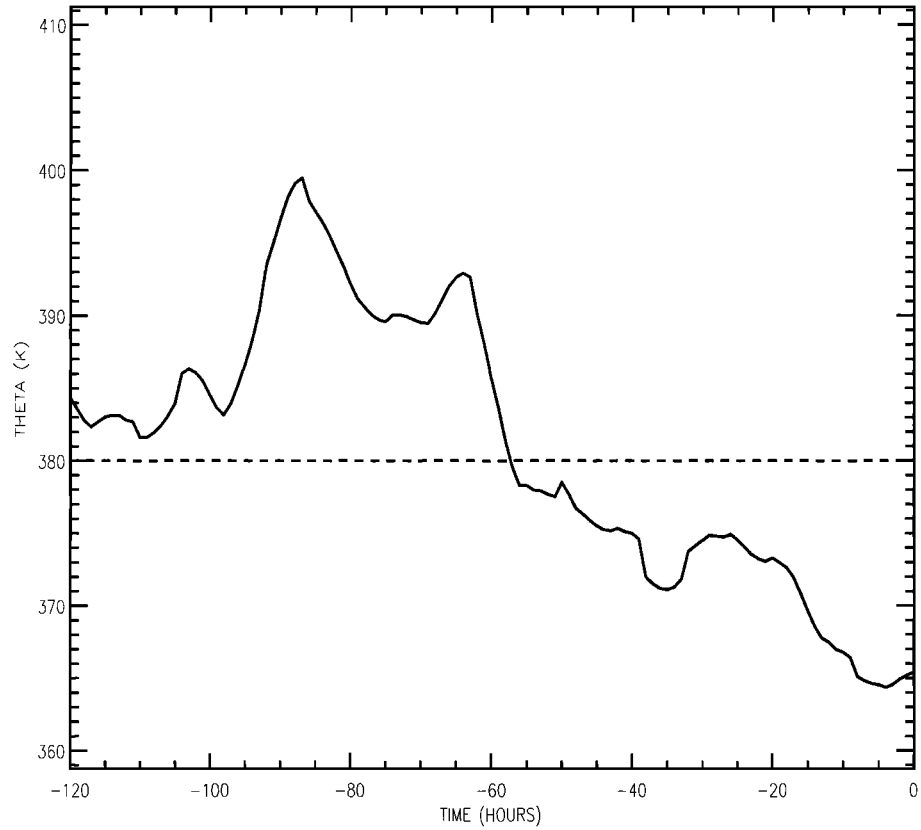

Figure 5. Potential temperature evolution along a trajectory from the cluster of sounding 12 starting in a layer at 110 hPa (see Plate 4). Time equal to 0 is the starting point of the trajectory (March 24), and time equal to −120 is the endpoint of the trajectory (March 19).

ECMWF model. We therefore believe it is more likely that STE has taken place due to shear-induced differential advection possibly preceded by CAT. ECMWF PV maps illustrate the stripping of laminae from the STJ in several cases.

However, stratospheric PV signatures along the trajectories were not always found. This does not necessarily imply that the air cannot be of stratospheric origin. There can be other reasons for a lack of conservation of a PV signal along the trajectory. If stratospheric air is mixed into the troposphere by CAT, then a pronounced PV signal would be lacking. Furthermore, even if the trajectory is perfect, one should realize that the PV is a grid box value. Thus, even if high PV laminae are present in the grid box, the PV signal will probably be suppressed by grid box averaging. Another reason could be that during transport the PV signature disappears rapidly due to absorption of solar radiation. In this case the chemical signature would remain unaffected. This may be especially important for thin layers in the tropics.

Only a few of the laminae do not seem to originate from the STJ but rather from the ITCZ. Yet also for these layers there are indications of a stratospheric origin in the PV maps (not shown). This implies that either the trajectories are wrong, which is likely near convection, or the exchange mechanism involves the ITCZ rather than the STJ. Overshooting clouds in the ITCZ can entrain stratospheric air into the turret [*Danielsen*, 1982]. Radiative and evaporative cooling cause the mixed air mass to sink back to the troposphere. Overshooting clouds also generate buoyancy waves in regions around the ITCZ [*Potter and Holton*, 1995; *Danielsen*, 1993]. These can cause STE, although this does not explain the observed horizontal orientation of the laminae. Finally, ozone production due to lightning associated with deep convection may also play a role. Further analyses will be needed in future.

Our results do not point to preferred latitudes for these stratospherically influenced layers. Rather, we have shown that the upper tropospheric laminae can be transported quasi-horizontally quite far away from the STJ into the deep tropics. To our knowledge, stratospheric influences in the form of thin layers with high O_3 concentrations close to the tropical tropopause have not been discussed in the literature before. The O_3 mixing ratios in the laminae close to the equator were as high as those close to the STJ, suggesting that mixing is not as important as for the midtropospheric O_3 maxima, in which mixing ratios were lower than those of the upper tropospheric laminae. Probably, the midtropospheric maxima undergo stronger influences from convection and turbulence.

Future work should concentrate on the frequency and distribution of these intrusions into the tropical troposphere and on aspects such as seasonal variability and interannual variability. Statistical analysis and chemistry-transport simulations should be performed in order to estimate the magnitude of the contribution of these intrusions to the total tropospheric O_3 budget in the tropics.

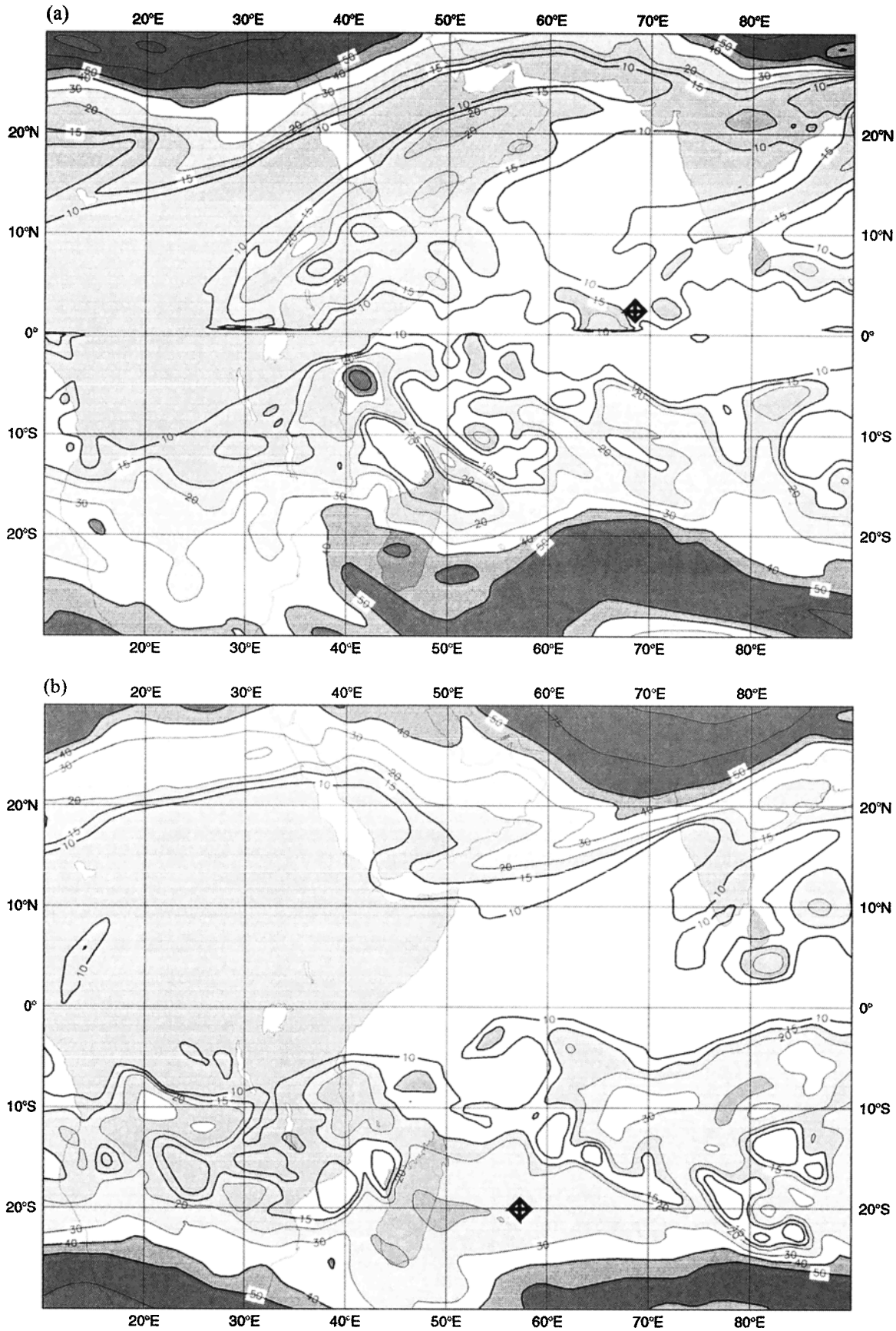

Figure 6. ECMWF potential vorticity (in 0.1 PVU. 1 PVU = 10^{-6} m^2 K kg^{-1} s^{-1}) at 100 hPa. The location of the profiles is given by a symbol. (a) March 24, 0600 UTC (sounding 12; 2.4°N/68.5°E) and (b) March 13, 1200 UTC (sounding 7; 20.1°S/57.3°E).

Acknowledgments. The authors would like to thank Rinus Scheele from the Royal Netherlands Meteorological Institute (KNMI) for his assistance with the back trajectory model. Furthermore, we thank Peter Siegmund from the KNMI for his critical review of the paper. We also thank the anonymous reviewers for their constructive comments on the paper. This work was supported by the Netherlands National Science Foundation (NWO).

References

Ambaum, M. H. P., Large-scale dynamics of the tropopause, Ph.D. thesis, Eindhoven Univ., Eindhoven, Netherlands, 1997.

Appenzeller, C., and J. R. Holton, Tracer lamination in the stratosphere: A global climatology, *J. Geophys. Res.*, *102*, 13,555–13,569, 1997.

Appenzeller, C., H. C. Davies, and W. A. Norton, Fragmentation of stratospheric intrusions, *J. Geophys. Res.*, *101*, 1435–1456, 1996.

Baldy, S., G. Ancellet, M. Bessafi, A. Badr, and D. Lan Sun Luk, Field observations of the vertical distribution of tropospheric ozone at the island of Reunion (southern tropics), *J. Geophys. Res.*, *101*, 23,835–23,849, 1996.

Baray, J. L., G. Ancellet, F. G. Taupin, M. Bessafi, S. Baldy, and P. Keckhut, Subtropical tropopause break as a possible stratospheric source of ozone in the tropical troposphere, *J. Atmos. Terr. Phys.*, *60*, 27–36, 1998.

Browell, E. V., et al., Large-scale air mass characteristics observed over western Pacific during summertime, *J. Geophys. Res.*, *101*, 1691–1712, 1996.

Cammas, J.-P., S. Jacoby-Koaly, K. Suhre, R. Rosset, and A. Marenco, Atlantic potential vorticity barrier as seen by Measurements of Ozone by Airbus In-Service Aircraft (MOZAIC) flights, *J. Geophys. Res.*, *103*, 25,681–25,693, 1998.

Chameides, W. L., The photochemical role of tropospheric nitrogen oxides, *Geophys. Res. Lett.*, *5*, 17–20, 1978.

Chatfield, R. B., J. A. Vastano, L. Li, G. W. Sachse, and V. S. Connors, The great African plume from biomass burning: Generalizations from a three-dimensional study of TRACE A carbon monoxide, *J. Geophys. Res.*, *103*, 28,059–28,077, 1998.

Crutzen, P. J., Photochemical reactions initiated by and influencing ozone in unpolluted tropospheric air, *Tellus*, *26*, 47–57, 1974.

Crutzen, P. J., L. E. Heidt, J. P. Krasnec, W. H. Pollock, and W. Seiler, Biomass burning as a source of atmospheric gases CO, H2, N2O, CH3Cl and COS, *Nature*, *282*, 253–256, 1979.

Crutzen, P. J., A. C. Delany, J. Greenberg, P. Haagenson, L. Heidt, R. Lueb, W. Pollock, W. Seiler, A. Wartburg, and P. Zimmerman, Tropospheric chemical composition measurements in Brazil during the dry season, *J. Atmos. Chem.*, *2*, 233–256, 1985.

Danielsen, E. F., A dehydration mechanism for the stratosphere, *Geophys. Res. Lett.*, *9*, 605–608, 1982.

Danielsen, E. F., In situ evidence of rapid, vertical, irreversible transport of lower tropospheric air into the lower tropical stratosphere by convective cloud turrets and by larger-scale upwelling in tropical cyclones, *J. Geophys. Res.*, *98*, 8665–8681, 1993.

De Laat, A. T. J., M. Zachariasse, G. J. Roelofs, P. van Velthoven, R. R. Dickerson, K. P. Rhoads, S. J. Oltmans, and J. Lelieveld, Tropospheric ozone distribution over the Indian Ocean during spring 1995 evaluated with a chemistry-climate model, *J. Geophys. Res.*, *104*, 13,881–13,894, 1999.

Fabian, P., and P. G. Pruchniewicz, Meridional distribution of ozone in the troposphere and its seasonal variations, *J. Geophys. Res.*, *82*, 2063–2073, 1977.

Fenn, M. A., et al., Ozone and aerosol distributions and air mass characteristics over the South Pacific during the burning season, *J. Geophys. Res.*, *104*, 16,197–16,212, 1999.

Fishman, J., S. Solomon, and P. J. Crutzen, Observational and theoretical evidence in support of a significant in situ photochemical source of tropospheric ozone, *Tellus*, *31*, 432–446, 1979.

Fishman, J., C. E. Watson, J. C. Larsen, and J. A. Logan, The distribution of tropospheric ozone determined from satellite data, *J. Geophys. Res.*, *95*, 3599–3617, 1990.

Fishman, J., K. Fakhruzzaman, B. Cros, and D. Nganga, Identification of widespread pollution in the Southern Hemisphere deduced from satellite analyses, *Science*, *252*, 1693–1696, 1991.

Folkins, I., M. Loewenstein, J. Podolske, S. J. Oltmans, and M. Profitt, A barrier to vertical mixing at 14 km in the tropics: Evidence from ozonesondes and aircraft measurements, *J. Geophys. Res.*, *104*, 22,095–22,102, 1999.

Greenberg, J. P., P. R. Zimmerman, L. Heidt, and W. Pollock, Hydrocarbon and carbon monoxide emissions from biomass burning in Brazil, *J. Geophys. Res.*, *89*, 1350–1354, 1984.

Heckley, W. A., Systematic errors of the ECMWF operational forecasting model in tropical regions, *Q. J. R. Meteorol. Soc.*, *11*, 709–738, 1985.

Holton, J. R., and J. Lelieveld, Stratosphere-troposphere exchange and its role in the budget of tropospheric O_3, *NATO ASI Ser.*, *135*, 173–190, 1996.

Intergovernmental Panel on Climate Change (IPCC), *Climate Change 1994—Radiative Forcing of Climate Change and an Evaluation of the IPCC IS92 Emission Scenarios*, edited by J. T. Houghton et al., 339 pp., Cambridge Univ. Press, New York, 1995.

Kennedy, P. J., and M. A. Shapiro, Further encounters with clear air turbulence in research aircraft, *J. Atmos. Sci.*, *37*, 986–993, 1980.

Kley, D., P. J. Crutzen, H. G. J. Smit, H. Vömel, S. J. Oltmans, H. Grassl, and V. Ramanathan, Observations of near-zero ozone concentrations over the convective Pacific: Effects on air chemistry, *Science*, *274*, 230–233, 1996.

Kley, D., H. G. J. Smit, H. Vömel, H. Grassl, V. Ramanathan, P. J. Crutzen, S. Williams, J. Meywerk, and S. J. Oltmans, Tropospheric water vapor and O_3 cross sections in a zonal plane over the central equatorial Pacific, *Q. J. R. Meteorol. Soc.*, *123*, 2009–2040, 1997.

Koppmann, R., A. Khedim, J. Rudolph, D. Poppe, M. O. Andrea, G. Helas, M. Welling, and T. Zenker, Emissions of organic trace gases from savanna fires in southern Africa during the 1992 Southern African Fire Atmosphere Research Initiative and their impact on the formation of tropospheric ozone, *J. Geophys. Res.*, *102*, 18,879–18,888, 1997.

Krishnamurti, T. N., H. E. Fuelberg, M. C. Sinha, D. Oosterhof, E. L. Bensman, and V. B. Kumar, The meteorological environment of the tropospheric ozone maximum over the tropical South Atlantic Ocean, *J. Geophys. Res.*, *98*, 10,621–10,641, 1993.

Lelieveld, J., and P. J. Crutzen, Role of deep cloud convection in the ozone budget of the troposphere, *Science*, *264*, 1759–1761, 1994.

Logan, J. A., J. J. Prather, S. C. Wofsy, and M. B. McElroy, Tropospheric chemistry: A global perspective, *J. Geophys. Res.*, *86*, 7210–7254, 1981.

Mandal, T. K., D. Kley, H. G. J. Smit, S. K. Srivastav, S. K. Peshin, and A. P. Mitra, Vertical distribution of ozone over the Indian Ocean (15°N–15°S) during First Field Phase INDOEX-1998, *Curr. Sci.*, *76*, 938–943, 1999.

Newell, R. E., Z.-X. Wu, Y. Zhu, W. Hu, E. V. Browell, G. L. Gregory, G. W. Sachse, J. E. Collins Jr., K. K. Kelly, and S. C. Liu, Vertical fine-scale atmospheric structure measured from NASA DC-8 during PEM-West A, *J. Geophys. Res.*, *101*, 1943–1960, 1996.

Newell, R. E., V. Thouret, J. Y. N. Cho, P. Stoller, A. Marenco, and H. G. J. Smit, Ubiquity of quasi-horizontal layers in the troposphere, *Nature*, *398*, 316–319, 1999.

Pepler, S. J., G. Vaughan, and D. A. Cooper, Detection of turbulence around jet streams using a VHF radar, *Q. J. R. Meteorol. Soc.*, *124*, 447–462, 1998.

Pickering, K. E., A. M. Thompson, J. R. Scala, W.-K. Tao, J. Simpson, and M. Garstang, Photochemical ozone production in tropical squall line convection during NASA Global Tropospheric Experiment/Amazon Boundary Layer Experiment 2A, *J. Geophys. Res.*, *96*, 3099–3114, 1991.

Piotrowicz, S. R., R. A. Rasmussen, K. J. Hanson, and C. J. Fischer, Ozone in the boundary layer of the equatorial Atlantic Ocean, *Tellus, Ser. B*, *41*, 314–322, 1989.

Potter, B. E., and J. R. Holton, The role of monsoon convection in the dehydration of the lower tropical stratosphere, *J. Atmos. Sci.*, *52*, 1034–1050, 1995.

Price, C., and D. Rind, Modeling global lightning distributions in a general circulation model, *Mon. Weather Rev.*, *122*, 1930–1939, 1994.

Randriambelo, T., J. L. Baray, S. Baldy, P. Bremaud, and S. Cautenet, A case study of extreme tropospheric ozone contamination in the tropics using in situ, satellite, and meteorological data, *Geophys. Res. Lett.*, *26*, 1287–1290, 1999.

Roelofs, G.-J., J. Lelieveld, H. G. J. Smit, and D. Kley, Ozone production and transports in the tropical Atlantic region during the biomass burning season, *J. Geophys. Res.*, *102*, 10,637–10,651, 1997.

Scheele, M. P., P. C. Siegmund, and P. F. J. van Velthoven, Sensitivity of trajectories to data resolution and its dependence on the starting point: In or outside a tropopause fold, *Meteorol. Appl.*, *3*, 267–273, 1996.

Shapiro, M. A., Further evidence of the mesoscale and turbulent structure of upper level jet stream-frontal zone systems, *Mon. Weather Rev.*, *106*, 1100–1111, 1978.

Shapiro, M. A., Turbulent mixing within tropopause folds as a mechanism for the exchange of chemical constituents between the stratosphere and troposphere, *J. Atmos. Sci.*, *37*, 994–1004, 1980.

Smit, H. G. J., and D. Kley, JOSIE: The 1996 WMO international intercomparison of ozone sondes under quasi flight conditions in the environmental simulation chamber at Jülich, *Tech. Doc. 296*, World Meteorol. Org., Geneva, 1998.

Smit, H. G. J., S. Gilge, and D. Kley, Ozone profiles over the Atlantic Ocean between 36°S and 52°N in March/April 1987 and September/October 1988, *Jul. Ber. 2567*, Forsch. Jülich, Jülich, Germany, 1991.

Smit, H. G. J., W. Sträter, D. Kley, and M. H. Profitt, The evaluation of ECC-ozone sondes under quasi flight conditions in the environmental simulation chamber at Jülich, in *Proceedings of Eurotrac Symposium 1994*, edited by P. M. Borell et al., pp. 349–353, SPB Acad., The Hague, Netherlands, 1994.

Suhre, K., J.-P. Cammas, P. Nédelec, R. Rosset, A. Marenco, and H. G. J. Smit, Ozone-rich transients in the upper equatorial Atlantic troposphere, *Nature*, *388*, 661–663, 1997.

Taupin, F. G., M. Bessafi, S. Baldy, and P. J. Bremaud, Tropospheric ozone above the southwestern Indian Ocean is strongly linked to dynamical conditions prevailing in the tropics, *J. Geophys. Res.*, *104*, 8057–8066, 1999.

Thompson, A. M., et al., Ozone over southern Africa during SAFARI-92/TRACE A, *J. Geophys. Res.*, *101*, 23,793–23,807, 1996.

Wu, Z., R. E. Newell, Y. Zhu, B. E. Anderson, E. V. Browell, G. L. Gregory, G. W. Sachse, and J. E. Collins Jr., Atmospheric layers measured from the NASA DC-8 during PEM-West B and comparison with PEM-West A, *J. Geophys. Res.*, *102*, 28,353–28,365, 1997.

Zahn, A., C. A. M. Brenninkmeijer, M. Maiss, D. Scharffe, P. J. Crutzen, M. Hermann, J. Heintzenberg, H. Fischer, J. W. M. Cuijpers, and P. F. J. van Velthoven, Identification of extratropical two-way troposphere-stratosphere mixing based on CARIBIC measurements of O_3, CO, and ultrafine particles, *J. Geophys. Res.*, *105*, 1527–1535, 2000.

H. Kelder, P. F. J. van Velthoven, and M. Zachariasse, Climate Research and Seismology Division/Atmospheric Composition Research, KNMI, P.O. Box 201, 3730 AE De Bilt, Netherlands. (zacharia@knmi.nl)

J. Lelieveld, Institute for Marine and Atmospheric Research (IMAU), Utrecht University, Princetonplein 5, 3584 CCUtrecht, Netherlands.

T. K. Mandal, National Physical Laboratory, Dr. K. S. Krishnan Road, New Delhi 110-012, India.

H. G. J. Smit, Institute for Chemistry of the Polluted Atmosphere (ICG-2), Research Centre Jülich, P.O. Box 1913, D-52425 Jülich, Germany.

(Received August 12, 1999; revised January 27, 2000;
accepted February 2, 2000.)